Precision Determination of Source Location with the HEGRA IACT System

M. Panter, G. Pühlhofer

Max - Planck - Institut für Kernphysik, P. O. Box 103980, D-69029 Heidelberg, Germany

Abstract

The HEGRA collaboration is operating a stereoscopic system of four imaging atmospheric Cherenkov telescopes. The stereoscopic view of TeV air showers allows to reconstruct the direction of individual γ primary particles with an accuracy of better than $0.1°$. The impact point can be measured within 15 m. The position of a point source of sufficient flux can be determined within $0.01°$.

1. Introduction

The imaging Cherenkov technique has proven the most powerful tool for the detection of air showers induced by TeV γ-rays. Several sources have been detected in the last few years (Weekes, 1996; Cawley and Weekes, 1996).

A Cherenkov telescope uses a mirror to project the Cherenkov light emitted by the air shower particles into a camera. The camera consists of photomultipliers which record the light flash, efficiently rejecting night-sky background photons by short gating times. The image represents a 2-dimensional projection of the shower. Its shape is used to discriminate between γ-ray - and hadron induced showers which cause a background signal of 99.9% of the total rate. Its position in the camera determines an area on the sky where the primary came from.

The common analysis technique for single-telescope data (Hillas, 1985; Punch, 1992; Petry, 1996) is mainly applicable to the search for point sources. The α parameter - the angle between the vector from the image center of gravity to the image of a candidate point source, and the image axis - is used to select events pointing to the source. In such analyses, telescope mispointing can be tolerated up to $\approx 0.1°$, without drastic loss in performance (Petry, 1996).

Stereoscopic viewing of showers yields far more detailed and unambiguous information about each event. It allows to determine the origin of the primary γ particle with an accuracy of better than $0.1°$. The shower core is defined as the virtual impact point of the primary onto the ground. It can be reconstructed within 15 meters. The energy resolution and the identification of the primary are improved significantly. By averaging over many events, source locations can be determined with subarcminute accuracy (Akerlof, 1991; Daum et al., 1997; Aharonian et al., 1997a; 1997b).

The HEGRA collaboration has built six Imaging Atmospheric Cherenkov Telescopes (Aharonian, 1993), of which four run as a stereoscopic system.

2. Telescope mounts and tracking

Each telescope of the HEGRA IACT system has an azimuthal mount with 30 mirrors arranged in the Davies-Cotton design (Davies and Cotton, 1957). The total mirror area is A = 8.5 m^2, the focal length is f = 4.9 m. The camera is mounted in the primary focus, and consists of 271 photomultipliers in a hexagonal matrix. Its field of view is 4.3°; each pixel covers 0.25°.

The telescope axes are driven by stepper motors; one step turns by 1.3". The positions are monitored by shaft encoders with a resolution of 1.3'. Tracking is computer controled; the algorithm uses a combination of calculated driving velocity and position feedback of the shaft encoders to steer the motors. This keeps the telescopes on track within ±1 shaft encoder tick.

The optical quality of a telescope is measured by the spot size caused by a point source at infinity, such as a star. The resulting point spread function should be small compared to the pixel size, but this means that the image of a star cannot be localized to better than the pixel size. Obviously the pointing accuracy needs an improved calibration.

Since pointing deviations translate directly into deviations of the reconstructed shower directions the pointing accuracy should be about one order of magnitude better than the air shower reconstruction accuracy $\leq 0.1°$ (Daum, 1997; Aharonian et al., 1997a; 1997b).

Pointing corrections should be understood in terms of a model of the mainly mechanical error sources. Such a description allows to reliably interpolate the corrections in between a finite set of calibration points. One can monitor the time variation of the relevant parameters of mount and drive, and may even be able to cure problems at their origin.

3. Pointing calibration

The pointing calibration by star images needs dedicated measurements for each star, so-called *point runs*, where the star is focused in the camera center where the spot is regular. The star image is then scanned across the central pixel, following a two-dimensional grid with spacings which are smaller than both the pixel size and the point spread function.

The current procedure for point runs represents an evolution of earlier techniques such as described in Mirzoyan et al., 1994. A typical scan takes about 15 min. The resulting distribution of current in the central pixel is proportional to the integral of the star's image over the pixel surface. Its center determines the center of the star image and therefore the telescope pointing relative to the star. This information is used to correct the pointing determined with the shaft encoder values. The steepness of the transitions at the pixel border allows to estimate the width of the point spread function.

A typical point run provides an accuracy of better than 0.01°. To derive a calibration which is valid for the complete hemisphere a set of pointruns has to cover the whole sky. Due to the azimuthal mount the telescope can be driven in two modes called *normal* and *reverse* (telescope turned across the zenith), therefore the hemisphere must be examined twice.

The minimum number of pointruns is determined by the number of required parameters to describe the deviations. Experience shows that at least 30 pointruns are needed for a new calibration. For further checks of pointing performance the dataset may be reduced.

4. Modeling of pointing deviations

Various types of misalignments were considered as causes for the measured deviations. The most prominent effects are the non-vertical alignment of the azimuth axis, the non-perpendicular alignment of the altitude relative to the azimuth axis, shaft encoder non-linearities and zero-point offsets, the shift of the camera center with respect to the optical axis of the telescope and the bending of telescope mount components. The influence of some of these parameters can be demonstrated by plotting horizontal respectively vertical deviation versus either azimuth or altitude while fixing the other coordinate. Two of the possible four plots are shown.

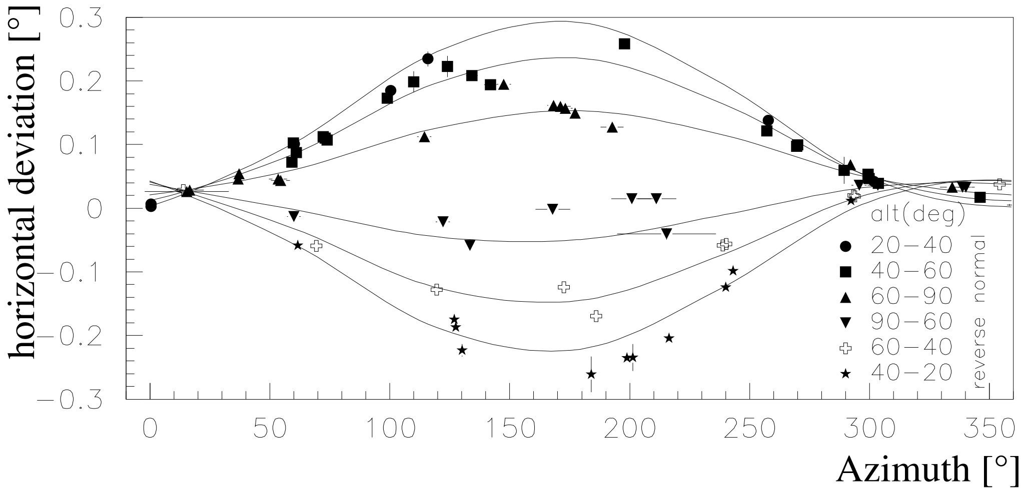

Fig. 1: Horizontal deviation vs. azimuth while applying six altitude slices.

In Fig. 1 the horizontal deviation is plotted versus azimuth. Besides a small mean offset the main effect here is a harmonic modulation with a period of 360°. This can be interpreted as an error of the azimuth shaft encoder; therefore the horizontal deviation decreases with increasing altitude - at the zenith an error in the azimuth value is obviously without consequences.

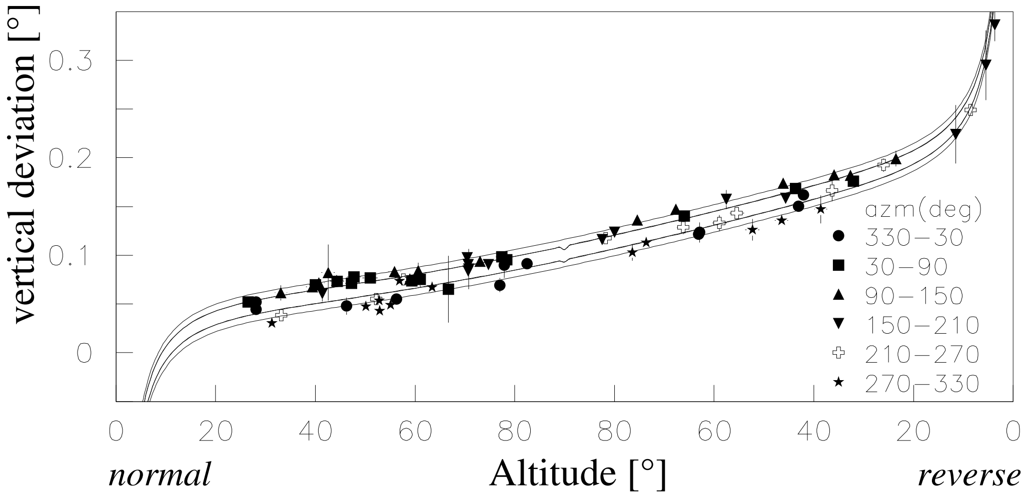

Fig. 2: Vertical deviation vs. altitude while applying six azimuthal slices.

In Fig. 2 the vertical deviation is plotted versus altitude. For all azimuth slices a common trend is visible which is interpreted as bending of parts of the telescope mount. This leads to a deviation in the vertical direction which depends on the altitude position. The small differences at different azimuth positions are caused by the non-vertical alignment of the azimuth axis.

At small altitudes atmospheric refraction becomes visible, causing a steep variation of pointing deviations with altitude.

All the sources of pointing deviations, including atmospheric refraction, are summarized in a model where their amplitudes and, where applicable, their phases are treated as free pa-

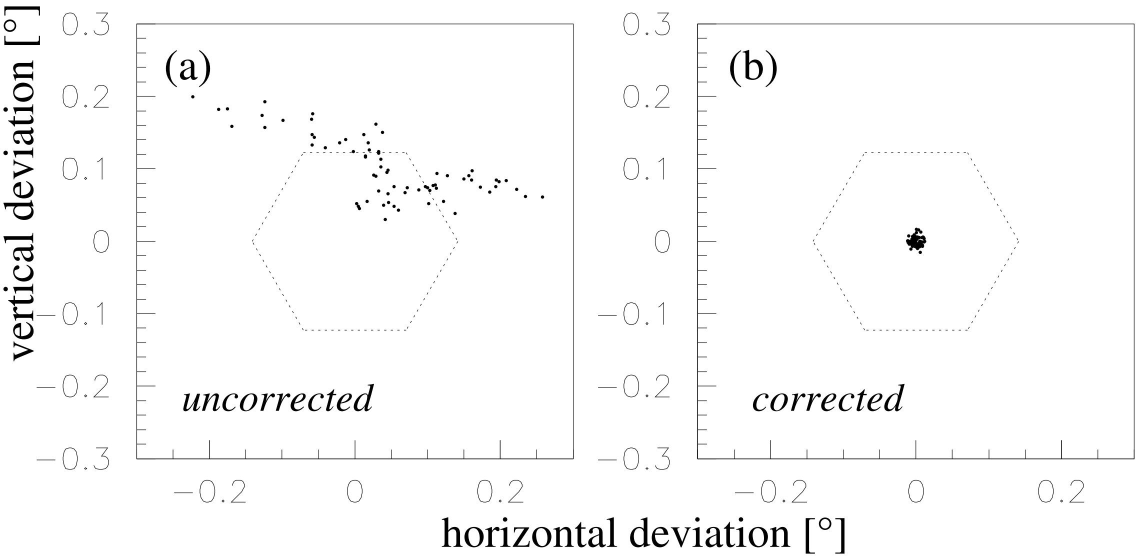

Fig. 3: The measured deviations are shown in the camera system (a) without correction, (b) after correction. The outline of the central pixel is superimposed.

rameters (Pühlhofer et al., 1997). The parameters are determined from a fit to the set of measured pointing deviations. The model can then be used to interpolate corrections between calibration points. As a measure of the quality and consistency of the model, Fig. 3 summarizes the pointing deviations before (a) and after (b) the correction function is applied. After corrections, the rms pointing error in both the horizontal and vertical directions is about 0.005°, with a mean consistent with zero. The number of fit parameters (11) is significantly smaller than the number of measured points, each of which provides two coordinates, (2×71 in the dataset used here, about 2×30 in standard new calibrations), hence this result is by no means trivial, and provides a genuine check of the model.

5. Results and Application to Air Showers

The correction functions were determined for all four telescopes of the HEGRA stereoscopic system. Provided that the calibration points are reasonably spread across the sky, each of the correction terms has its own distinctive signature, and the correlations between fit parameters are modest. Repeated complete calibrations demonstrated that the correction parameters are reproducable, and rather stable in time, unless hardware changes intervene.

For all four telescopes, the correction scheme succeeded in reducing pointing errors to the order of 0.01° or less. The observed pointing deviations before correction are typically of the order of the pixel size. Therefore tracking is good enough to maintain a source reasonably centered within the field of view, and it is sufficient to apply pointing corrections offline. This implies the great advantage that the calibration can be delayed to a convenient time, even after hardware changes which affect the pointing.

The pointing calibration was tested with two point sources of known positions, the Crab pulsar, a plerion at a distance of 8.5 kpc and Markarian 501, a blazar at a redshift of $z \approx 0.03$. Analysis procedures and first results concerning the Crab observations were reported in Daum et al., 1997, still using preliminary and incomplete pointing corrections. The results on γ-ray emission from Mkn 501, as summarized in Aharonian et al., 1997c, used the final corrections.

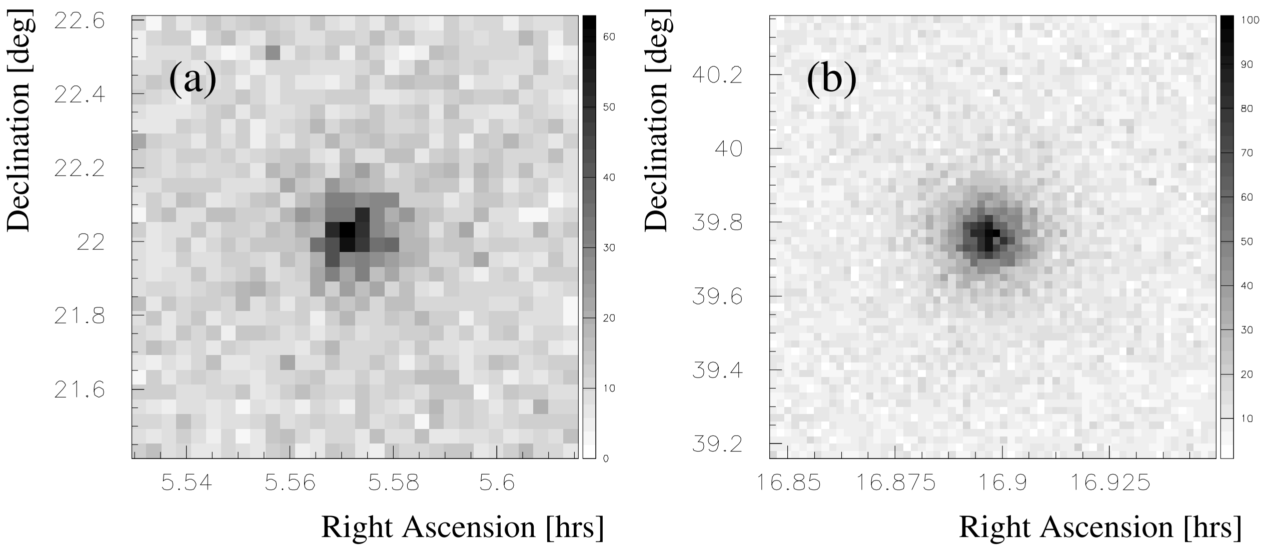

Fig. 4: Excess of γ-ray candidate events from the direction of the Crab nebula (a) and the blazar Mkn 501 (b), after subtraction of the uniform cosmic-ray background.

Figs. 4 (a) and (b) show the distribution of excess events in celestial coordinates, after subtraction of the uniform cosmic-ray background as determined from the surrounding regions. The positions of the γ-ray sources were determined from fits of two-dimensional Gaussian distributions to the excess. The relevant parameters of the data sets and the fit results concerning the source positions are summarized in Table 1.

Source	Crab	Mkn 501
Observation period	12/96 - 2/97	3/97 - 5/97
On-source time / Observation mode	24.3 hrs / normal	62.7 hrs /reverse
Radio source position of current epoch		
ra	5.5725 hrs	16.8963 hrs
dec	22.013°	39.764°
Angular distance radio source - γ-ray source		
along ra	$0.007° \pm 0.007°$	$0.006° \pm 0.007°$
along dec	$0.007° \pm 0.007°$	$0.002° \pm 0.007°$
(Gaussian) angular resolution	0.09°	0.09°

Table 1: Data sets and results of the analysis of Crab and Mkn 501 data. The errors given for the angular distances represent our estimate on systematical errors, the statistical errors are significantly smaller.

Neither the resolution for individual events nor the determination of source locations is limited by the pixel size of 0.25°: Most of the Crab data and all Mkn 501 data was taken with the source displaced from the camera center by $\pm 0.5°$ in declination, which causes a continuous movement of the source position in the cameras during data taking. The pointing corrections are applied *offline*. So during data taking each camera is differently displaced from the nominal position.

The reconstructed positions differ from the radio source positions by less than 1 arcminute which is in good agreement with the expected pointing accuracy. The corresponding errors are estimated from the residuals of the telescope pointing after correction. The angular resolution is well below 0.1°

6. Summary

The HEGRA IACT system provides a spatial resolution of a new quality in TeV γ-ray astronomy and even in γ-ray astronomy in general. The origin of an individual γ-ray can be reconstructed with an accuracy of better than 0.1°. The position of a point source of sufficient flux can be determined within 0.01°. To achieve this pointing quality a new calibration procedure for IACTs had to be established. It uses a set of ≥ 30 pointing calibration measurements distributed over the complete sky. These determine the parameters of correction functions to model the mechanical misalignments of the four telescopes of the HEGRA stereoscopic system. The correction functions work for the complete range in azimuth and altitude.

The precise localization of γ-ray sources allows better identification of counterparts in other wavebands, and may ultimately allow the precise mapping of extended sources.

7. Acknowledgements

The support of the German Ministry for Research and Technology BMBF and of the Spanish Research Council CYCIT is gratefully acknowledged. We thank the Instituto de Astrofisica de Canarias for the use of the site and for providing excellent working conditions. We thank the other members of the HEGRA CT groups, who participated in the construction, installation, and operation of the telescopes. We gratefully acknowledge the technical support staff of Heidelberg, Kiel, Munich, and Yerevan.

References

Aharonian, F.,1993, in Proceedings of the Int. Workshop "Towards a Major Atmospheric Cherenkov Detector II", Calgary, ed. R. C. Lamb, 81
Aharonian, F. et al., 1997a, in Astropart. Phys. 6, 343
Aharonian, F. et al., 1997b, in Astropart. Phys. 6, 369
Aharonian, F. et al., 1997c, preprint astro-ph/9706019, and A&A letters, in press
Akerlof, C. W., et. al., 1991, in Astrophys. J. 377, L97
Cawley, M. F. and Weekes, T. C., 1996, in Experimental Astronomy 6, 7
Davies, J. M., and Cotton, E. S., 1957, in J. Solar Energy Sci. and Eng. 1, 16
Daum, A. et al., 1997, preprint astro-ph/9704098, and Astropart. Phys., in press
Hillas, A. M., 1985, in Proc. 19th ICRC, La Jolla, Vol. 3, 445
Mirzoyan, R. et al., 1994, in Nucl. Instr. Meth. A351, 513
Petry, D., et al., 1996, in Astron. Astrophys. 311, L13
Pühlhofer G. et al., 1997, submitted to Astropart. Phys.
Punch, M. et al., 1992, in Nature 358, 447.
Weekes,T. C.,1996, in Space Science Rev. 75, 1